Reaction Kinetics, Mechanisms and Catalysis (2023) 136:2039–2051
https://doi.org/10.1007/s11144-023-02437-5

Synergetic effect of Pt–Pd bimetallic nanoparticle on $MgAl_2O_4$ support in hydrogen production from decalin dehydrogenation

Mingsheng Luo[1,2] · Fengli Wang[1,2] · Qinglong Liu[1,2] · Wenda Li[1] · Changke Shao[1,2] · Xinyue Liu[1,2] · Bohan Ai[1,2]

Received: 10 April 2023 / Accepted: 14 June 2023 / Published online: 26 June 2023

Abstract

In the present study, $MgAl_2O_4$ carriers were synthesized by the alcohol-heating method, and the effects of Pt loading and Pt/Pd molar ratio on decalin dehydrogenation activity were investigated systematically. The results showed that the size of Pt nanoparticle in the Pt/$MgAl_2O_4$ catalysts was closely related to the Pt loading and the optimum Pt loading was 3 wt% in the decalin dehydrogenation. The PtPd bimetallic catalyst with a Pt/Pd molar ratio of 4:1 generated moderate interactions and enhanced the catalytic performance. The superior catalytic performance of the 1 wt% $Pt_4Pd_1/MgAl_2O_4$ catalyst was mainly due to the synergistic effect of bimetallic Pt–Pd nanoparticles.

Keywords Liquid-phase hydrogen storage · Decalin dehydrogenation · $MgAl_2O_4$ catalyst support · Platinum-palladium bimetallic catalyst

Introduction

Hydrogen is considered as an ideal clean energy carrier to replace fossil fuels [1–6]. However, the major challenge in hydrogen application is how to reversibly use the hydrogen carrier. High-pressure gaseous hydrogen storage requires significant external energy consumption and the high pressure poses great safety hazard. Compared with high-pressure gaseous hydrogen storage, cryogenic liquid-phase hydrogen storage has a higher bulk hydrogen storage density, but economic and safety issues limit its wide application. Compared with the above-mentioned

✉ Qinglong Liu
lql@bipt.edu.cn

1 College of New Materials and Chemical Engineering, Beijing Institute of Petrochemical Technology, Beijing 102617, China

2 Beijing Key Laboratory of Clean Fuels and Efficient Catalytic Emission Reduction Technology, Beijing 102617, China

hydrogen storage methods, liquid phase organic hydride hydrogen storage has many advantages such as high hydrogen storage density, economy and safety [7–10]. Decalin is a hydrogen carrier with high hydrogen storage density, and its mass hydrogen density (7.3 wt%) and molar hydrogen density (32.44 mol/L) are higher than the U.S. Department of Energy's criteria for decalin being one of the best hydrogen storage materials [11].

Exothermic hydrogenation of aromatic hydrocarbons is relatively easier to proceed than the endothermic dehydrogenation. Therefore, finding a suitable dehydrogenation catalyst is the key to develop the hydrogen storage technology of aromatics. For the dehydrogenation of decalin, researchers have conducted numerous studies on various catalysts. The active components of the catalysts can directly affect the catalytic performance of the decalin dehydrogenation. Pt, Pd or other noble metal catalysts are more common candidates for the decalin dehydrogenation [12, 13]. Suh et al. found that the dehydrogenation of decalin produce both naphthalene and tetralin in the same time. Pt-based catalysts generate higher activity in the process of decalin to tetralin, while Pd based catalysts are more conducive to the dehydrogenation of tetralin to naphthalene [14]. Chen et al. found that Pt generated strong electronic interactions with the $MgAl_2O_4$, forming a positively charged Pt, thus leading to the adsorption of the product on the Pt active site and achieving a higher decalin dehydrogenation activity [15]. Dehydrogenation is a complex process, and the synergistic effect of multi-components yields a beneficial effect on the dehydrogenation process. Qi et al. prepared a Pt-Ni bimetallic catalyst for the decalin dehydrogenation and found that the dehydrogenation activity of bimetallic catalysts was higher than that of corresponding monometallic catalysts. This may be attributed to the formation of Pt-Ni-Pt structure on the surface of bimetallic catalyst, and its hydrogenation activity was higher than that of corresponding single metal surface [16]. Suttisawat et al. investigated the effect of adding Sn to Pt-based catalysts on the decalin dehydrogenation performance [17]. It was found that Sn can provide electrons to Pt atoms, and this electronic effect could reduce sintering and agglomeration of Pt and inhibit hydrogenolysis and isomerization reactions, thus improving the activity and stability of Pt-based catalysts. Kariya et al. found that the addition of moderate amounts of Pd to Pt catalysts promoted the cyclohexane dehydrogenation process, which may be due to the electronic effect of the second metal [18].

The nature of the support also exerts an important influence on the activity of Pt-based catalysts. Martynenko et al. investigated the catalytic activity of Pt-based catalysts supported on Al_2O_3, amorphous SiO_2, mesoporous silica SBA-15 and MCM-48 for the catalytic decalin dehydrogenation [19]. Their results indicated that Pt/SBA-15 and Pt/MCM-48 had higher catalytic activity, due to the high specific surface area and sufficiently large pore volume to obtain enhanced dispersion of active sites. The main differences between different Pt-based catalysts are the size of Pt nanoclusters and the dispersion of the active phase. Recently, it is found that $MgAl_2O_4$ can be used as catalyst support in methane reforming [20, 21], alkane dehydrogenation [15, 22, 23], ammonia decomposition and other fields [24, 25], due to their high thermal stability, low coefficient of thermal expansion, as well as desired acid and base active centers. Bimetallic catalysts have attracted much attention in dehydrogenation research due to their excellent catalytic performance. So far

little research on the application of PtPd bimetallic catalyst prepared with $MgAl_2O_4$ support in dehydrogenation of decalin has been reported in the literature.

In this work, a series of Pt loading catalysts and PtPd bimetallic catalysts were prepared supported on $MgAl_2O_4$ for decalin dehydrogenation. The physicochemical properties of the samples were characterized with X-ray diffraction (XRD), N_2 isothermal adsorption desorption (BET), transmission electron microscopy (TEM), and H_2 temperature programmed reduction (H_2-TPR). The effects of Pt dispersion and the synergistic effect between Pt and Pd metals on the performance of decalin dehydrogenation catalysts were also systematically studied in this work.

Experimental

Catalyst preparation

Preparation of $MgAl_2O_4$ support material

$MgAl_2O_4$ was synthesized by alcohol-heating method. 0.01 mol magnesium nitrate hexahydrate and 0.02 mol aluminum isopropoxide were mixed in 30 mL of ethanol and stirred at 40 °C for 1 h. Then the turbid liquid was transferred to a Teflon autoclave and kept at a constant temperature of 150 °C for 12 h. The mixture was transferred to a beaker and dried in a 90 °C oven until the ethanol was completely volatilized. The solid powder was calcined in a muffle furnace and heated to 700 °C for 12 h at a heating rate of 5 °C/min.

Preparation of catalyst sample

Pt/$MgAl_2O_4$ catalysts were prepared by the excessive impregnation method. Using a series of different amount of 1 g/L $H_2PtCl_6{\cdot}6H_2O$ solution to impregnate the $MgAl_2O_4$ support for 2 h before each sample was dried at 80 °C in a rotary evaporator for 8 h.

PtPd/$MgAl_2O_4$ catalysts were also prepared by the excessive impregnation method. 1 g/L of $H_2PtCl_6{\cdot}6H_2O$ solutions and 2.5 g/L of $PdCl_2$ solutions were added into the support at 1/4, 1/1, 4/1 and 6/1 Pt/Pd molar ratio and 1 wt% of total metal loading, and then the suspension was stirred at room temperature for 2 h. The subsequent steps were the same as the preparation method of Pt/$MgAl_2O_4$. The catalysts with different molar ratios of Pt and Pd were separately prepared as 1 wt%Pt_xPd_y/$MgAl_2O_4$ (1 wt% total metal load is the ratio of the total mass of Pt and Pd to the mass of catalyst, and x/y is the molar ratio of Pt and Pd, i.e., 0/1, 1/4, 1/1, 4/1, 6/1, 1/0).

Catalyst and support material characterization

All catalysts are characterized after reduction, and the support is directly characterized. The N_2 adsorption–desorption isotherms were determined at −196 °C by

BELSORP-max (MicrotracBEL, Corp.). The BET surface area was determined by the Brunauer–Emmett–Teller equation, the pore volume was reckoned from N_2 adsorption amount at a relative pressure of $P/P_0 = 0.996$, and the pore size distribution curves were confirmed from the desorption branch using the Barrett-Joyner-Halenda (BJH) model. The XRD patterns of the samples were recorded on a Japan Rigaku Ultima IV diffractometer at a scanning speed of 4 min^{-1} in the range of 10°–90°. The phase was identified by comparing the diffraction patterns with the Joint Committee on Powder Diffraction Standards (JCPDSs). H_2-TPR was conducted on a BELCAT-II (MicrotracBEL, Corp.) chemisorption instrument, 50 mg of sample was placed in the quartz tube and pretreated with high purity Ar (30 mL/min) at 300 °C for 1 h before cooled to 50 °C. The sample was reduced in a 10% H_2/Ar gas flow from 50 to 900 °C at a heating rate of 10 °C/min. The amount of H_2 consumption was quantified using CuO as internal standard. TEM image was obtained on JEMF-200 Electron Microscope.

Catalytic activity evaluation

At a certain reaction temperature, with the variation of the ratio of decalin volume to catalyst mass, three different reaction states could occur in the dehydrogenation reaction: suspended state, superheated liquid-film state and sand bath state [10, 18]. This study selected the reaction state of superheated liquid-film.

Decalin dehydrogenation was carried out in a 50 mL three-necked flat-bottomed flask. The samples were reduced with flowing H_2 at 300 °C for 3 h. In a standard experiment, 0.3 g catalyst was put into the bottom of the flask to form a thin layer, and 1 mL decalin was added to the catalyst to ensure that the catalyst was wet. Then the experimental device was flushed with N_2 for 20 min to remove O_2. When the reactor was heated to the reaction temperature in a heating jacket to start the reaction. Evolved hydrogen was collected into a gas burette and quantified volumetrically. Reaction rates were obtained from the evolved amount of gaseous hydrogen continuously. In addition, blank experiments were carried out on the $MgAl_2O_4$ supports to eliminate the catalytic effect of supports on decalin dehydrogenation.

Results and discussion

Effect of Pt loading on the decalin dehydrogenation

Fig. 1 showed the XRD patterns of the catalysts with different Pt loading. For the catalyst with 3 wt% or lower loading, the X-ray diffraction pattern shows only the $MgAl_2O_4$ peak, indicating that the Pt species were highly dispersed and the average size of Pt nanoparticles was lower than the detection limit of XRD. However, when the loading continued to increase to 4 or 5 wt%, the diffraction peaks of Pt particles appeared and the intensity of the diffraction peaks gradually increased, indicating that the aggregation of Pt species occurred and resulted in the formation of larger Pt

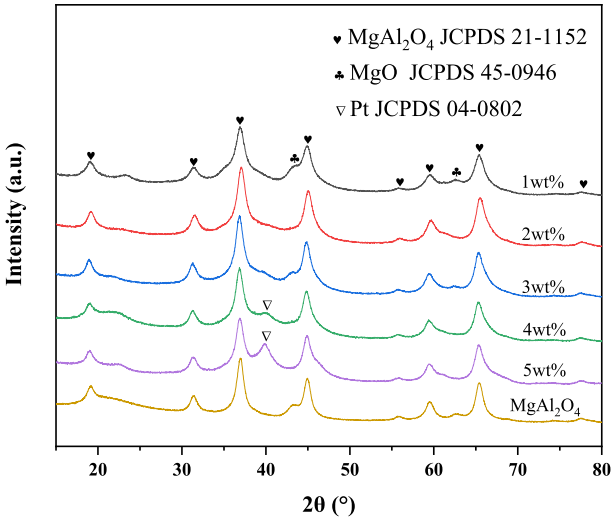

Fig. 1 XRD patterns of the Pt/$MgAl_2O_4$ catalysts with different Pt loading and $MgAl_2O_4$

particles with increasing the Pt loading. Besides, the peaks at 42.9° and 62.3° were attributable to MgO.

TEM analysis was used to investigate the Pt nanoparticles size in the catalysts. Fig. 2 showed the TEM morphology of representative samples and the corresponding histograms of the size distribution of Pt nanoparticles. The Pt aggregates in 1 wt%Pt/$MgAl_2O_4$ appeared to be amorphous rather than crystals with well-defined edges because the Pt content was very low and there were not enough atoms to form

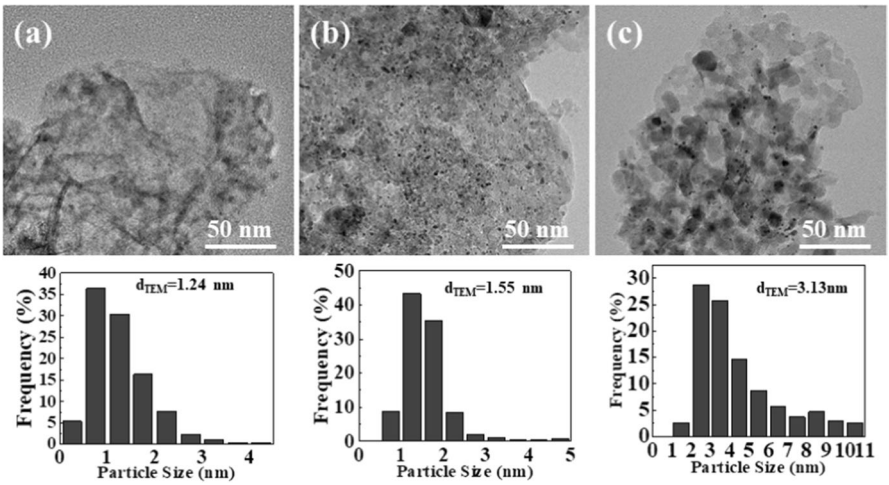

Fig. 2 TEM images of the **a** 1 wt%Pt/$MgAl_2O_4$, **b** 3 wt%Pt/$MgAl_2O_4$ and **c** 5 wt%Pt/$MgAl_2O_4$ catalysts

crystals [26]. Similar processes were observed for various support-loaded Pt and other noble metals [27]. For the 3 wt% Pt/$MgAl_2O_4$ catalyst, the tiny Pt nanoparticles were highly dispersed on the surface of $MgAl_2O_4$, and the particle size was concentrated at 1–2 nm. With increasing Pt loading, significant agglomeration of Pt particles can be observed in 5 wt% Pt/$MgAl_2O_4$, and the particle size was widely distributed in the range of 2–10 nm.

Nitrogen adsorption–desorption experiments were carried out to investigate the specific surface area and pore characteristics of the catalysts with different Pt loadings. Type IV adsorption–desorption isotherms with H3 hysteresis loops were observed for all samples and the samples were typically ordered mesoporous materials as shown in Fig. S1a. This can be further explained by the wide size of 2–40 nm as shown in Fig. S1b. Thus, the presence of a large number of mesoporous structures in Pt/$MgAl_2O_4$ is further evidenced by the BET results for Pt/$MgAl_2O_4$ listed in Table S1. The specific surface area of the catalyst was reduced to different degrees by adding Pt to the support, which can be attributed to the incorporation of Pt nanoparticles into the support. It was obvious that Pt loading had no obvious effect on the pore size distribution of the catalyst, and the synthesized catalyst maintained the mesoporous structure.

The reducibility of catalysts with different Pt loadings was investigated using H_2-TPR measurements. As shown in Fig. 3, for all catalysts, two peaks were observed at about 480 and 520 °C. The peaks at lower temperature of 480 °C were attributed to the reduction of PtO and PtO_2 while the peak at 520 °C may be due to the inorganic platinum complex formed with the separated platinum oxide. It was obvious from the peaks that at the reduction temperature of 600 °C, all Pt can be successfully reduced to the metal Pt. In addition, H_2-consumption peak was also observed in $MgAl_2O_4$ support, corresponding to the reduction of $MgAl_2O_4$.

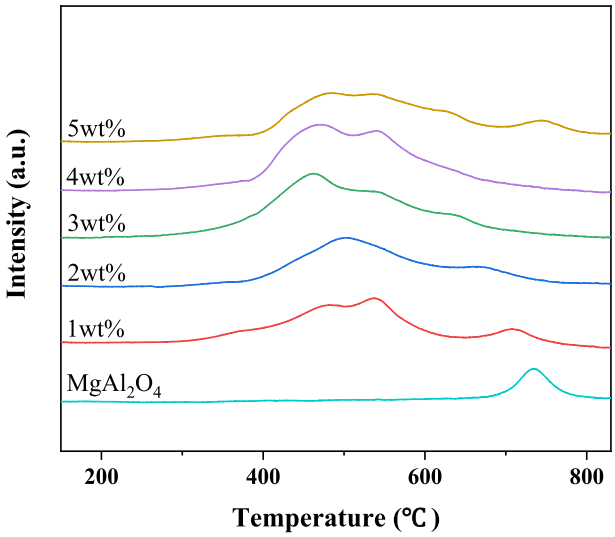

Fig. 3 H_2-TPR profiles of $MgAl_2O_4$ support and Pt/$MgAl_2O_4$ catalysts with different Pt loading

With the increase of Pt loading, the peaks shift to lower temperatures. This indicates that the excessive loading led to the aggregation of Pt particles and the formation of larger Pt particles that were more conducive to reduction. Higher reduction temperature was necessary for catalysts with less Pt loading. It showed that there was a strong interaction between Pt nanoparticles and $MgAl_2O_4$, resulting in the high dispersion of Pt nanoparticles. This phenomenon was highly consistent with TEM results, where the Pt nanoparticle size of 3 wt%Pt/$MgAl_2O_4$ was concentrated at 1–2 nm. Basically, it was smaller than the Pt particle size supported on the traditional supports such as Al_2O_3 with only 2 wt% Pt loading [19]. These results indicated that $MgAl_2O_4$ can stabilize the Pt nanoparticles due to the strong metal-support interaction.

The effect of Pt loading on the dehydrogenation performance of decalin over Pt/$MgAl_2O_4$ catalyst was investigated to obtain the hydrogen yield and the H_2 production rate of catalysts with different Pt loading as shown in Fig. 4. Under the conditions of this experiment, the maximum theoretical hydrogen production is 32 mmol. When the Pt loading was 1 wt%, the final hydrogen production was only 15.9 mmol. With the increase of Pt loading, the activity of the catalysts increased significantly. When the Pt loading reached 3 wt%, the final hydrogen production reached 18.4 mmol. However, with the further increase of Pt loading, the activity of the catalysts decreased. These results indicated that a maximum hydrogen yield can be obtained over a catalyst with 3 wt% of Pt.

For all active components of heterogeneous catalysts, the size of metal nanoparticles and their dispersion on the support are critical to its catalytic performance. As shown from the TEM results, the Pt particle size in 3 wt%Pt/$MgAl_2O_4$ was concentrated at 1–2 nm, and no significant nanoparticle aggregation occurred. The highly dispersed Pt nanoparticles in 3 wt%Pt/$MgAl_2O_4$ are likely the main active sites for

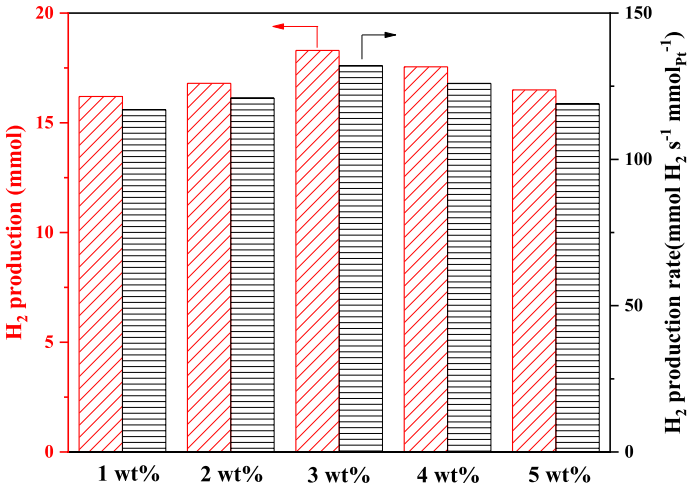

Fig. 4 H_2 productivity and the H_2 production rate for Pt/$MgAl_2O_4$ catalysts with different Pt loading. Experimental conditions: catalyst dosage = 0.3 g, addition amount of decalin = 1 mL, reaction time: 2.5 h, reaction temperature: 260 °C

high decalin dehydrogenation activity. For the catalysts with very low Pt loading, the singularly dispersed Pt atoms may play the dominant role on the catalyst. With the increasing Pt loading, larger Pt nanoparticles were formed, and the catalytic efficiency gradually decreased.

The number of active center is related to Pt loading. However, with the further increase of Pt loading, the activity of the catalysts decreased, which was related to the dispersion and the structural change of Pt species. Fig. S2 showed the XRD patterns of the 5 wt% catalyst before and after the reaction. The results indicated that the used catalyst had stronger Pt diffraction peaks and narrower half-peak widths than the fresh catalyst, suggesting some Pt particle aggregation in this sample during the reaction process. These results illustrated that too high Pt loading may cause agglomeration of Pt particles, thus reducing the exposed active sites and damaging the catalytic activity.

Effect of PtPd bimetal on decalin dehydrogenation

The XRD patterns of 1 wt%Pt/$MgAl_2O_4$, 1 wt%Pd/$MgAl_2O_4$ and PtPd bimetallic catalysts with different Pt to Pd molar ratios were shown in Fig. S3. All samples show characteristic peaks attributed to $MgAl_2O_4$ (JCPDS No.21–1152) at 19.0°, 31.3°, 36.8°, 44.7°, 55.7°, 59.4°, 65.2° and 77.3°, corresponding to (111), (220), (311), (400), (422), (511) and (533) crystal planes. In addition, there was no characteristic diffraction peak attributed Pt or Pd particles, which may be due to the low noble metal loading (1 wt%) or small metal particle size.

The N_2 adsorption isotherms and pore size distribution of different catalysts were presented in Fig. S4, and the structural properties of the newly calcined catalysts were shown in Table 1. Per IUPAC classification, all catalysts exhibited a type IV adsorption–desorption isotherm with an H3 hysteresis loop, which was typical of mesoporous materials [28]. With the addition of Pt and Pd, the specific surface area, total pore volume and mean pore diameter decrease to different degrees likely due to the doping of noble metal nanoparticles into the mesoporous carrier.

To determine the state of PtPd species in PtPd bimetallic catalysts, the metal particle size was studied using TEM. As shown in Fig. S5, large particle size and some

Table 1 Textural properties of different catalysts

Catalysts	S_{BET}[a] (m^2/g)	V_p[b] (cm^3/g)	D_m[c] (nm)	Particle size (nm)
1 wt%Pd/$MgAl_2O_4$	267	0.86	12.89	–
1 wt%Pt_1Pd_4/$MgAl_2O_4$	212	0.73	13.66	1.51 ± 0.7 nm
1 wt%Pt_1Pd_1/$MgAl_2O_4$	220	0.73	13.37	–
1 wt%Pt_4Pd_1/$MgAl_2O_4$	216	0.75	13.85	1.32 ± 0.5 nm
1 wt%Pt_6Pd_1/$MgAl_2O_4$	233	0.74	12.77	–
1 wt%Pt/$MgAl_2O_4$	307	0.8	11.3	1.24 ± 0.5 nm

[a]S_{BET} is the specific surface area calculated by BET method

[b]V_p is the total pore volume

[c]D_m is the mean pore diameter

agglomerations can be observed for 1 wt%$Pt_1Pd_4/MgAl_2O_4$ while smaller metal particle size and relatively uniformly dispersed metals on the surface of the $MgAl_2O_4$ support observed for 1 wt%$Pt_4Pd_1/MgAl_2O_4$ sample. The metal particle size of 1 wt%Pt/$MgAl_2O_4$ was more uniform and smaller. With the decrease of Pt/Pd molar ratio, more agglomerates appeared in the images, which is mainly due to the different nucleation growth mechanisms of Pt and Pd metal nanoparticles [29]. Similar phenomena have been reported by some other researchers [30]. In order to further clarify the distribution of Pt and Pd species, energy dispersive x-ray spectroscopy (EDS) was performed on 1 wt%$Pt_4Pd_1/MgAl_2O_4$ samples. As shown in Fig. S5h–j, Pt and Pd species were uniformly distributed as tiny nanoparticles. The uniform metal dispersion facilitated more metal atoms to be exposed and thus more catalytic active sites to participate in the catalytic reaction.

H_2-TPR is a powerful tool to study the reducibility properties of catalysts and to reveal the interaction between the support and the loaded metals. Fig. S6 showed the TPR profiles of the fresh catalysts. The TPR curve of the single metal 1 wt%Pt/$MgAl_2O_4$ catalyst had a main reduction peak at 535 °C and a small peak at about 710 °C. The TPR curves of 1 wt%Pd/$MgAl_2O_4$ catalysts showed two reduction peaks at 400 and 550 °C. The bimetallic PtPd catalysts showed one large reduction peak near 535 °C that cannot be attributed to the reduction of some specific species. It was reasonable to attribute this peak to the co-reduction of Pt and Pd. The change in the width of the reduction peak indicated that Pt was co-reduced with Pd, suggesting a strong interaction between the metals that may form an alloy. The presence of Pd altered the reduction performance of the PtPd catalyst. H_2-TPR profiles indicated that there may be a strong interaction between the Pt and Pd components.

The catalytic activity of monometallic 1 wt%Pt/$MgAl_2O_4$, 1 wt%Pd/$MgAl_2O_4$ and PtPd bimetallic samples were tested for the decalin dehydrogenation. The results in Fig. 5 showed that the ratio of Pt to Pd had an important effect on the decalin dehydrogenation performance of the catalysts. The catalytic activity of the bimetallic catalysts for the decalin dehydrogenation showed a trend of increasing and then decreasing with the increase of the relative content of Pd. When the molar ratio of Pt to Pd was 4:1, the catalyst showed the highest catalytic activity with a hydrogen yield of 18.6 mmol. The TEM results showed that the size of PtPd nanoparticles with Pt/Pd molar ratio of 4:1 were small and uniformly dispersed on the surface of $MgAl_2O_4$ support. It can be inferred that the difference of catalyst microstructure is an important factor for the difference of catalytic performance. In addition, the TPR results also indicated a strong interaction between Pt and Pd, which might result in the synergistic effect in the decalin dehydrogenation.

Actually, the decalin dehydrogenation reaction can be divided into two processes. First, the dehydrogenation of decalin generates the intermediate product tetralin, which further converted to naphthalene [31]. Kim et al. found that Pt catalyst was more conducive to the conversion of decalin to tetralin, while Pd was more conducive to the conversion of tetralin to naphthalene [14]. For this purpose, tetralin dehydrogenation experiments were carried out on the different catalysts, and Fig. 6 showed the comparative hydrogen yield of the reaction for 2.5 h at 260 °C, 0.3 g catalyst and 1 mL tetralin. With the addition of Pd, the catalyst exhibited superior catalytic performance, and the H_2 production of 1 wt%Pd/$MgAl_2O_4$ reached 9.8 mmol. The experimental results

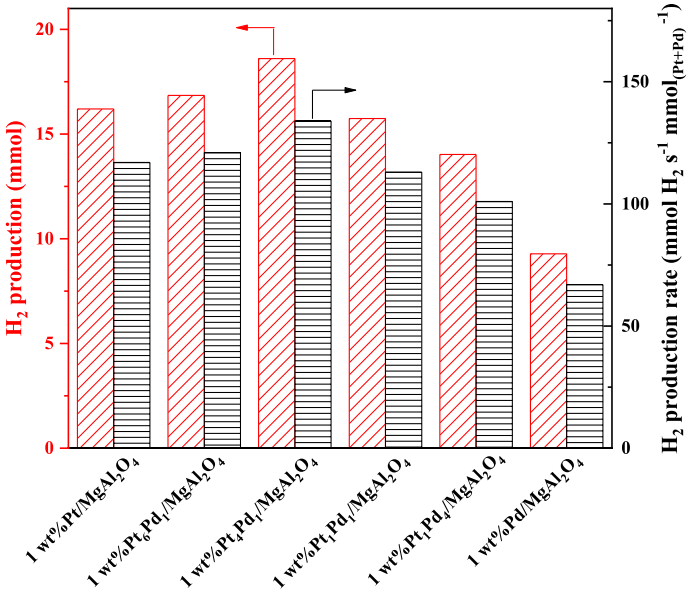

Fig. 5 H_2 production and H_2 production rate of catalysts

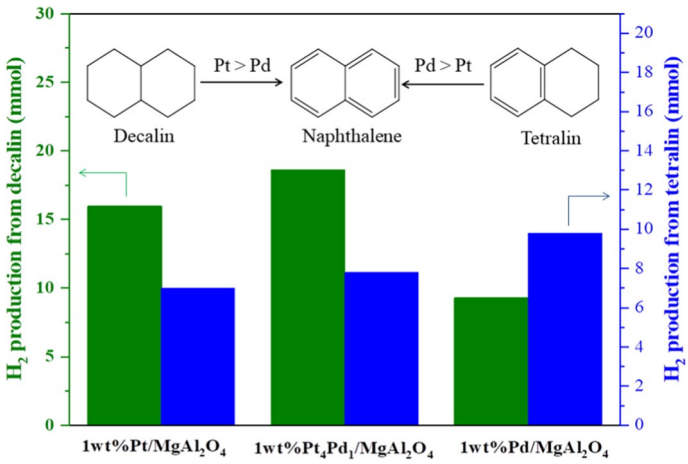

Fig. 6 Comparison of H_2 production of decalin and tetralin on different catalysts. Experimental conditions: catalyst dosage = 0.3 g, addition amount of decalin = 1 mL, reaction time: 2.5 h, reaction temperature: 260 °C

showed an important influence of the active component on the decalin dehydrogenation process, which was in agreement with other literature [14]. Martynenko [19] and Park [32] et al. examined in detail the effect of Pt-based catalysts on the dehydrogenation process of decahydronaphthalene and compared the product composition by gas chromatography. Therefore, the composition of the product composition was further

investigated by gas chromatography, and the results were shown in Table S2. It can be seen that Pt is more favorable for the conversion of decalin to naphthalene, while Pd is more favorable for the conversion of decalin to tetralin. However, each literature has different reaction conditions, resulting in different hydrogen yields. The red part in Table S2 is the data of this experiment. It can be seen that the H_2 production in this experiment is relatively high.

The above results showed that the decalin dehydrogenation was a complex process and affected by many factors. The addition of moderate amount of Pd promoted the increase of H_2 production. These suggested that a significant Pt–Pd synergy exists in the $MgAl_2O_4$ supported PtPd bimetallic catalysts for enhanced the catalytic activity. However, excessive Pd led to the decrease in H_2 production. Therefore, the modification of suitable catalysts was particularly important for the decalin dehydrogenation process.

Experimental conditions: catalyst dosage = 0.3 g, addition amount of decalin = 1 mL, reaction time: 2.5 h, reaction temperature: 260 °C.

Conclusions

In summary, an efficient $MgAl_2O_4$ supported Pt monometallic and PtPd bimetallic catalyst were prepared for decalin dehydrogenation. Experimental results proves that 3 wt% is the optimum Pt loading. 1 wt%$Pt_4Pd_1/MgAl_2O_4$ exhibited excellent decalin dehydrogenation performance. The $MgAl_2O_4$ support and bimetallic PtPd nanoparticles played a key role in improving the catalytic performance. The catalytic reaction was accelerated due to the dispersion effect of $MgAl_2O_4$ support on PtPd bimetallic nanoparticles. In particular, the synergistic effect of PtPd bimetallic nanoparticles promoted the dehydrogenation process of decalin and improved the hydrogen yield. This study will help to design and modify the efficient decalin dehydrogenation catalyst, and is of great significance to the application of hydrogen storage technology using liquid-phase organic hydrocarbons.

Supplementary Information The online version contains supplementary material available at https://doi.org/10.1007/s11144-023-02437-5.

Funding This work was supported from the National Natural Science Foundation of China (22202013), Beijing Education Committee Science and Technology Project (KM202110017010) and the special fund from the Beijing Institute of Petrochemical Technology (Grant No. 15031862004-1).

Declarations

Competing interest The authors declare that they have no known competing financial interests or personal relationships that could have appeared to influence the work reported in this paper.

References

1. Muzzio M, Lin H, Wei K, Guo X, Sun S (2020) Efficient hydrogen generation from ammonia borane and tandem hydrogenation or hydrodehalogenation over AuPd nanoparticles. ACS Sustain Chem Eng 8:2814–2821. https://doi.org/10.1021/acssuschemeng.9b06862
2. Zou H, Guo F, Luo M, Yao Q, Lu Z (2020) $La(OH)_3$-decorated NiFe nanoparticles as efficient catalyst for hydrogen evolution from hydrous hydrazine and hydrazine borane. Int J Hydrogen Energ 45:11641–11650. https://doi.org/10.1016/j.ijhydene.2020.02.074
3. Zhang L, Ji L, Yao Z, Yan N, Chen L (2019) Facile synthesized Fe nanosheets as superior active catalyst for hydrogen storage in MgH_2. Int J Hydrogen Energ 44:21955–21964. https://doi.org/10.1016/j.ijhydene.2019.06.065
4. Dai X, Cao T, Lu X, Bai Y, Qi W (2023) Tailored Pd/C bifunctional catalysts for styrene production under an ethylbenzene oxidative dehydrogenation assisted direct dehydrogenation scheme. Appl Catal B Environ 324:122205. https://doi.org/10.1016/j.apcatb.2022.122205
5. Wang Z, Liu G, Zhang X (2023) Efficient and stable Pt/CaO-TiO_2-Al_2O_3 for the catalytic dehydrogenation of cycloalkanes as an endothermic hydrocarbon fuel. Fuel 331:125732. https://doi.org/10.1016/j.fuel.2022.125732
6. Zhang D, Zong P, Wang J, Gao H, Guo J, Wang J, Wang Y, Tian Y, Qiao Y (2023) Catalytic dehydrogenation cracking of crude oil to light olefins by structure and basicity/acidity adjustment of bifunctional metal/acid catalysts. Fuel 334:126808. https://doi.org/10.1016/j.fuel.2022.126808
7. Lang C, Jia Y, Yao X (2020) Recent advances in liquid-phase chemical hydrogen storage. Energy Storage Mater 26:290–312. https://doi.org/10.4028/www.scientific.net/AMR.512-515.1438
8. Du J, Zhao R, Jiao G (2013) The short-channel function of hollow carbon nanoparticles as support in the dehydrogenation of cyclohexane. Int J Hydrogen Energ 38:5789–5795. https://doi.org/10.1016/j.ijhydene.2013.03.064
9. Biniwale R, Rayalu S, Devotta S, Ichikawa M (2008) Chemical hydrides: a solution to high capacity hydrogen storage and supply. Int J Hydrogen Energ 33:360–365. https://doi.org/10.1016/j.ijhydene.2007.07.028
10. Saito Y, Aramaki K, Hodoshima S, Saito M, Shono A, Kuwano J, Otake K (2008) Efficient hydrogen generation from organic chemical hydrides by using catalytic reactor on the basis of superheated liquid-film concept-ScienceDirect. Chem Eng Sci 63:4935–4941. https://doi.org/10.1016/j.ces.2007.11.036
11. Satyapal S, Petrovic J, Read C, Thomas G, Ordaz G (2007) The U.S. department of energy's national hydrogen storage project: progress towards meeting hydrogen-powered vehicle requirements. Catal Today 120:246–256. https://doi.org/10.1016/j.cattod.2006.09.022
12. Sattler J, Ruiz-Martinez J, Santillan-Jimenez E, Weckhuysen B (2014) Catalytic Dehydrogenation of Light Alkanes on Metals and Metal Oxides. Chem Rev 114(20):10613–10653. https://doi.org/10.1021/cr5002436
13. Chen S, Pei C, Sun G, Zhao Z, Gong J (2020) Nanostructured catalysts toward efficient propane dehydrogenation. Accounts Mater Res 1:11. https://doi.org/10.1021/accountsmr.0c00012
14. Suh Y-W, Kim T, Wan P, Ji H, Kyeounghak J (2017) Different catalytic behaviors of Pd and Pt metals in decalin dehydrogenation to naphthalene. Catal Sci Technol 7:3728–3735. https://doi.org/10.1039/c7cy00569e
15. Tuo Y, Meng Y, Chen C, Lin D, Zhang J (2021) Partial positively charged Pt in Pt/$MgAl_2O_4$ for enhanced dehydrogenation activity. Appl Catal B-Environ 288:119996. https://doi.org/10.1016/j.apcatb.2021.119996
16. Qi S, Li Y, Yue J, Chen H, Yi C, Yang B (2014) Hydrogen production from decalin dehydrogenation over Pt-Ni/C bimetallic catalysts. Chinese J Catal 35:1833–1839. https://doi.org/10.1016/S1872-2067(14)60178-9
17. Suttisawat Y, Sakai H, Abe M, Rangsunvigit P, Horikoshi S (2012) Microwave effect in the dehydrogenation of tetralin and decalin with a fixed-bed reactor. Int J Hydrogen Energ 37:3242–3250. https://doi.org/10.1016/j.ijhydene.2011.10.111
18. Kariya N, Fukuoka A, Ichikawa M (2002) Efficient evolution of hydrogen from liquid cycloalkanes over Pt-containing catalysts supported on active carbons under "wet-dry multiphase conditions." Appl Catal A-Gen 233:91–102. https://doi.org/10.1016/S0926-860X(02)00139-4

19. Martynenko E, Pimerzin A, Savinov A, Verevkin S, Pimerzin A (2020) Hydrogen release from decalin by catalytic dehydrogenation over supported platinum catalysts. Top Catal 63:178–186. https://doi.org/10.1007/s11244-020-01228-9
20. Hadian N, Rezaei M (2013) Combination of dry reforming and partial oxidation of methane over Ni catalysts supported on nanocrystalline MgAl2O4. Fuel 113:571–579. https://doi.org/10.1016/j.fuel.2013.06.013
21. Jaiswar V, Katheria S, Deo G, Kunzru D (2017) Effect of Pt doping on activity and stability of Ni/$MgAl_2O_4$ catalyst for steam reforming of methane at ambient and high pressure condition. Int J Hydrogen Energ 42:18968–18976. https://doi.org/10.1016/j.ijhydene.2017.06.096
22. Tahier T, Mohiuddin E, Key D, Mdleleni M (2021) In-depth investigation of the effect of $MgAl_2O_4$ and SiO_2 support on sulfur promoted nickel catalysts for the dehydrogenation of propane- ScienceDirect. Catal Today 377:176–186. https://doi.org/10.1016/j.cattod.2020.12.028
23. Li J, Tong F, Li Y, Liu X, Guo Y, Wang Y (2022) Dehydrogenation of dodecahydro-N-ethylcarbazole over spinel supporting catalyst in a continuous flow fixed bed reactor. Fuel 321:124034. https://doi.org/10.1016/j.fuel.2022.124034
24. Qiu Y, Fu E, Gong F, Xiao R (2022) Catalyst support effect on ammonia decomposition over Ni/$MgAl_2O_4$ towards hydrogen production. Int J Hydrogen Energy 47:5044–5052. https://doi.org/10.1016/j.ijhydene.2021.11.117
25. Zehtab Salmasi M, Kazemeini M, Sadjadi S, Nematollahi R (2022) Spinel MgAl2O4 nanospheres coupled with modified graphitic carbon nitride nanosheets as an efficient Z-scheme photocatalyst for photodegradation of organic contaminants. Appl Surf Sci 585:152615. https://doi.org/10.1016/j.apsusc.2022.152615
26. Yan F, Zhao C, Yi L, Zhang J, Ge B, Zhang T, Li W (2017) Effect of the degree of dispersion of Pt over $MgAl_2O_4$ on the catalytic hydrogenation of benzaldehyde. Chinese J Catal 38:1613–1620. https://doi.org/10.1016/S1872-2067(17)62815-8
27. Kwak J, Hu J, Mei D, Yi CW, Kim D, Peden C, Allard L, Szanyi J (2009) Coordinatively unsaturated Al^{3+} centers as binding sites for active catalyst phases of platinum on γ-Al_2O_3. Science 325:1670–1673. https://doi.org/10.1126/science.1176745
28. Thommes M (2016) Physisorption of gases, with special reference to the evaluation of surface area and pore size distribution (IUPAC Technical Report). Pure Appl Chem 87:25. https://doi.org/10.1515/pac-2014-1117
29. Li H, Sun G, Qian J, Zhu M, Sun S, Qin X (2007) Synthesis of highly dispersed Pd/C electro-catalyst with high activity for formic acid oxidation. Electrochem Commun 9:1410–1415. https://doi.org/10.1016/j.elecom.2007.01.032
30. Wang W, Huang Q, Liu J, Zou Z, Hui Y (2008) One-step synthesis of carbon-supported Pd-Pt alloy electrocatalysts for methanol tolerant oxygen reduction. Electrochem Commun 10:1396–1399. https://doi.org/10.1016/j.elecom.2008.07.018
31. Bo W, Goodman D, Froment G (2008) Kinetic modeling of pure hydrogen production from decalin. J Catal 253:229–238. https://doi.org/10.1016/j.jcat.2007.11.012
32. Jiang N, Rao K, Jin M, Park S (2012) Effect of hydrogen spillover in decalin dehydrogenation over supported Pt catalysts. Appl Catal A-Gen 425:62–67. https://doi.org/10.1016/j.apcata.2012.03.001